JOURNAL OF SOLID STATE CHEMISTRY 54, 170–178 (1984)

X-Ray Absorption Spectroscopy of Transition-Metal Trichalcogenides

YOUICHI OHNO, KATSUICHI KANEDA, AND SHOZO OKADA

Department of Physics, Faculty of General Education, Utsunomiya University, Mine-machi 350, Utsunomiya 321, Japan

AND KIMIAKI HIRAMA

Department of Applied Physics, Faculty of Engineering, Utsunomiya University, Ishii-machi 2753, Utsunomiya, 321 Japan

Received November 21, 1983; in revised form March 12, 1984

The sulfur K and metal L_{III} absorption spectra of transition-metal trichalcogenides (TMTC's) were measured. The matrix element effect plays an important role in these spectra. It was considered that the structures up to 5 eV above the absorption edge reflect the chalcogen antibonding band, the metal nonbonding d_{z^2} band, and the metal d bands, and that the higher energy structures are derived from the metal s and p bands. The chalcogen antibonding band arises from chalcogen pairing and the metal d, s, and p bands are the mixture bands with chalcogen p orbitals. Evidence that shows that the lowest conduction band of the group IV TMTC's is the chalcogen antibonding band is presented. The overlap of the metal d and metal s bands is promoted by increasing the atomic number of chalcogen atoms.

Introduction

Transition-metal trichalcogenides (TMTC's) crystallize in layer-type structures with one-dimensional chains (*1*). We may consider a distorted bicapped prism as a basal element, a central metal atom being coordinated to the eight chalcogen atoms at the corners. The neighboring chains are displaced by one-half the prism height along the chain axis and linked together to form an extended layer. The bonding between the layers is due to the van der Waals force and the crystals can be easily cleaved. In this sense, TMTC's are layer compounds. However, the fact that the conductivity ratios σ_b/σ_a and σ_b/σ_c of $NbSe_3$ are 500 and 20, respectively, suggests that they would rather be regarded as a quasi-one-dimensional compound at least with respect to the electrical properties (*2, 3*). These features reflect the electronic band structures, especially the valence and conduction band structures near the Fermi level. Such a low dimensionality brings about the formation of the charge density waves and the metal–semiconductor transition associated with the Peierls instability (*4, 5*).

Energy band calculations have been carried out for some of these compounds by Bullett (*6–9*), Hoffmann *et al.* (*10*), and Myron *et al.* (*11*). The optical experiments have been done by many workers. The photoemission spectra, which give us information on both the core levels and the valence band structures, have been measured for

0022-4596/84 $3.00

TiS_3, ZrS_3, $ZrSe_3$, $HfSe_3$, NbS_3, TaS_3, $NbSe_3$, and $TaSe_3$ by Jellinek *et al.* (*12*), Margaritondo *et al.* (*13*), Endo *et al.* (*14–16*), and Zhao *et al.* (*17*). The reflectivity spectra have been measured systematically for the group IV compounds by Khumalo and Hughes (*18*) and Khumalo *et al.* (*19*), and the optical absorption has also been reported for TiS_3, ZrS_3, $ZrSe_3$, and HfS_3 by Grimmeiss *et al.* (*20*), Scharer and Shafer (*21*), Perluzzo *et al.* (*22*), and Kurita *et al.* (*23*), which give us information on the joint density of states and on the direct and indirect energy gaps. At present, however, the conduction band structures remain almost unknown.

This paper presents the sulfur K and metal L_{III} absorption spectra of TMTC's and we discuss the electronic band structures with the aid of the band calculations, the photoemission spectra, and the other optical spectra. We also investigate the band character from the comparison of the different kind of absorption spectra of the same compound.

Experiments

All the samples used here were prepared by a direct reaction of elements in stoichiometric amounts in evacuated silica ampoules. The synthetic conditions for the group IV compounds have been described in Ref. (*24*) in detail. The crystal structures and the lattice parameters were determined from X-ray powder patterns. It was possible to assign the Miller indices to all the diffraction peaks. The measurements of X-ray absorption spectra were done using a Yohan-type vacuum soft X-ray spectrometer having a Rowland circle with radius 30 cm. The sample was installed in the apparatus in the form of a thin film by rubbing fine powder onto a sheet of thin paper. The dispersing crystal was quartz with a $(10\bar{1}1)$ plane for S K absorption spectra and with a $(10\bar{1}0)$ plane for Zr L_{III} and Nb L_{III} absorption spectra, respectively. The spectra were obtained by step scanning with unit-step energies of 0.29, 0.27, and 0.32 eV for the S K, Zr L_{III}, and Nb L_{III} spectra, respectively. The experimental details have been described in previous papers (*25, 26*).

Results and Discussions

(*1*) *The Group IV Compounds*

We know that TiS_3, ZrS_3, and HfS_3, the group IV compounds, are the semiconductors with the indirect energy gaps of 0.9, 2.0, and 2.8 eV, respectively (*20–23*). Their S K absorption spectra are shown in Figs. 1, 2, and 3, together with the corresponding photoemission spectrum. The insets show the reflectivity spectra measured by Khumalo and Hughes (*18*).

Perluzzo *et al.* (*27*) found a donor impurity level of 0.2 eV below the conduction band of ZrS_3 and related it to a sulfur vacancy. The same result was obtained by Kurita *et al.* (*23*) who observed a broad luminescence band with a peak energy of 1.76 eV in the energy gap. If a sulfur vacancy gives rise to a shallow donor level in the other compounds in the same way, they would be n-type semiconductors, the Fermi level lying near the bottom of the conduc-

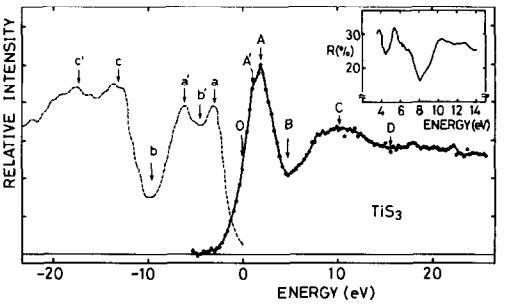

FIG. 1. S K absorption spectrum of TiS_3, together with the photoemission spectrum measured by Endo *et al.* (Ref. (*16*)). The full and dashed lines refer to the S K absorption and photoemission spectra, respectively. Inset is the reflectivity spectrum measured by Khumalo and Hughes (Ref. (*18*)).

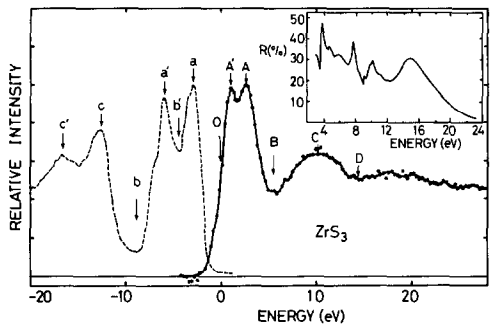

FIG. 2. S K absorption spectrum of ZrS_3, together with the photoemission spectrum measured by Jellinek *et al.* (Ref. (*12*)). The full and dashed lines refer to the S K absorption and photoemission spectra, respectively. Inset is the reflectivity spectrum measured by Khumalo and Hughes (Ref. (*18*)).

tion band. Therefore, it would be reasonable to fit the absorption edge to the position of the Fermi level determined from the photoemission studies and adopt it as the origin of the horizontal axis. The photon energy at the absorption edge (the midpoint of the initial rise of absorption) was 2468.8, 2468.9, and 2468.8 eV for TiS_3, ZrS_3, and HfS_3, respectively, which are in agreement with each other within the errors in contrast to the dichalcogenides (*26*).

We find that the initial rise of absorption of TiS_3 is not so sharp as that of the corresponding disulfide and of the other group IV TMTC's. It is known that TiS_3 crystallizes in the B-type structure with variable bond lengths between metal and chalcogen atoms (*28*). In this case, the different degrees of metal–chalcogen interactions occur, which give rise to the broadening of the energy bands and in turn the gentle slope of the initial rise of absorption.

As can be seen from the figures, all the absorption spectra can be separated into two parts; one is the large absorption structure up to about 5 eV above the edge and the other is the relatively broad structure at higher energies. The former structure has a shoulder at the lower energy side of the peak in TiS_3, but it splits into two or three peaks in ZrS_3 and HfS_3. The maximum intensity relative to the latter structure is higher than that of the corresponding disulfide, for example, the ratio is 1.5 and 1.1 for the titanium tri- and disulfides, respectively. Such a large intensity ratio has also been found for the group V and VI dichalcogenides in which the metal atoms are trigonal-prismatically coordinated to the chalcogen atoms (*26, 29*).

One of the present authors propose the band model in which the chalcogen pairs are included as a basal element and metal atoms are eightfold-coordinated to the chalcogen atoms at the corners of bicapped trigonal prisms (*30*). According to the model, the lower conduction band consists of the chalcogen antibonding $\sigma_u^*(p_x\text{-}p_x)$ band, the metal nonbonding d_{z^2} band and the metal d bands, and the upper conduction band consists of the metal s and p bands. The antibonding $\sigma_u^*(p_x\text{-}p_x)$ band is derived from the chalcogen pairs and the metal d, s, and p bands are the mixture bands with chalcogen p orbitals. Since a K absorption spectrum represents the p-like empty states, the absorption structures up to about 5 eV above the edge can be ascribed to the antibonding $\sigma_u^*(p_x\text{-}p_x)$ and the metal d bands, while the higher energy structure to the metal s and p bands.

The relative energy position of the antibonding $\sigma_u^*(p_x\text{-}p_x)$ band to the metal d bands

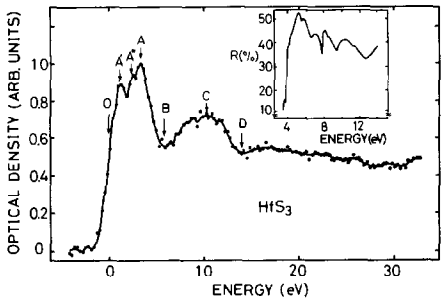

FIG. 3. S K absorption spectrum of HfS_3. Inset is the reflectivity spectrum measured by Khumalo and Hughes (Ref. (*18*)).

is varied both with the degree of the sulfur–pair interaction and with the energy difference between metal d and sulfur p levels. However, we may assign the main peak A to the metal d bands and the shoulder structure A′ in TiS_3 and the lower energy peak A′ in ZrS_3 and HfS_3 to the antibonding $\sigma_u^*(p_x\text{-}p_x)$ band, from the following reasons. (i) The sulfur–pair distance is larger in ZrS_3 and HfS_3 than in TiS_3, which gives rise to the lower energy shift of the antibonding $\sigma_u^*(p_x\text{-}p_x)$ band by reducing the bonding–antibonding energy gap. The metal d levels of ZrS_3 and HfS_3, on the other hand, lie at higher energies than that of TiS_3. As a result, the antibonding $\sigma_u^*(p_x\text{-}p_x)$ and the metal d bands are energetically lowered and raised, respectively, on going from TiS_3 to ZrS_3 or HfS_3. Then the variations of the spectra can be explained satisfactorily provided that the structure A′ is derived from the antibonding $\sigma_u^*(p_x\text{-}p_x)$ band and the structure A from the metal d bands. (ii) According to the band calculations of Bullett (*7*) and Myron *et al.* (*11*), the lowest conduction band of $ZrSe_3$ consists of the antibonding p band.

Although the energy position of the nonbonding d_{z^2} band cannot be determined from the S K absorption spectra due to the selection rules, it is possible that this band overlaps the antibonding $\sigma_u^*(p_x\text{-}p_x)$ band. Figure 4 shows the Zr L_{III} absorption spectra of zirconium trichalcogenides. These spectra consist of the main peak around 2–3 eV above the edge, followed by the extending absorption structures. The photon energies at the peak are in agreement with each other within the errors. The Zr L_{III} absorption spectrum of the trisulfide is different in shape from the corresponding S K spectrum. This is probably due to the selection rules in X-ray excitations described above. Since an L_{III} absorption spectrum represents the empty states with s and d symmetry, we could obtain information on the nonbonding d_{z^2} band in addition to the

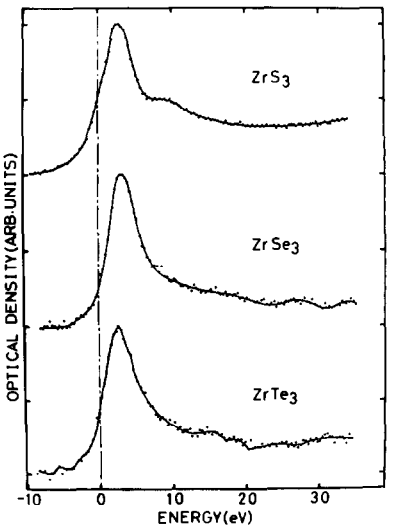

FIG. 4. Zr L_{III} absorption spectra of the zirconium trichalcogenides.

metal d bands. If the lower and the higher conduction bands consist of the antibonding $\sigma_u^*(p_x\text{-}p_x)$ band overlapping the nonbonding d_{z^2} band and the metal d bands, respectively, the intensity ratio of the lower to higher energy peak would be smaller for the Zr L_{III} absorption spectrum than for the S K absorption spectrum because the number of states per unit cell is four for both the antibonding $\sigma_u^*(p_x\text{-}p_x)$ band and the nonbonding d_{z^2} band but the metal d bands include a metal d character much more than a sulfur p character. We can observe a shoulder at the lower energy side of the main Zr L_{III} absorption peak and thus assign it to the nonbonding d_{z^2} band. The extending absorption structures at higher energies, on the other hand, can be ascribed to the metal s band or the higher s or d bands. As can be seen from Fig. 4, the metal s band overlaps the metal d bands, which is promoted with increasing the atomic number of chalcogen atoms.

The results obtained above are summarized:

(i) The lowest conduction band is the chalcogen antibonding $\sigma_u^*(p_x\text{-}p_x)$ band

which largely overlaps the nonbonding d_{z^2} band. The higher energy band is the metal d bands, the center of which lies at 2–3 eV above the Fermi level. The full bandwidth is about 4–5 eV.

(ii) The upper conduction band consists of the metal s and p bands. The s band overlaps the metal d bands and its center lies at about 6–7 eV above the Fermi level, while the p band lies around 10 eV above the Fermi level and the width is about 7 eV.

(iii) The overlap between the metal d and metal s bands develops with increasing the atomic number of chalcogen atoms.

The valence band structures are known from the photoemission spectra and can be separated into two large parts (see Figs. 1 and 2), i.e., the lower valence bands are derived primarily from sulfur s orbitals and the upper valence bands primarily from sulfur p orbitals, some of them having some metal d, s, and p character. The latter bands have been observed as two large peaks in X-ray photoemission spectra (*12, 14–16*), but as four or five peaks in ultraviolet photoemission spectra (*13, 17*). The bandwidth in a base is 6–8 eV.

The reflectivity spectra exhibit a large dip around 8 eV and a peak around 5 eV. As can be seen from Figs. 1 and 2, the peak separations between a and A′ and between a and A are about 4 and 5 eV, respectively. Since the peaks a and A are considered to be derived from the mixture bands of sulfur p and metal d orbitals, it is probable that the peak around 5 eV is caused by the allowed p–d and/or d–p transitions and the large dip around 8 eV originates from the exhaustion of the above transitions. The dip around 12 eV would, on the other hand, result from the exhaustion of the transitions from the upper valence bands to the metal d bands and the onset of the transitions from the lower valence bands. The other energy separations are tabulated in Table I. These spectra, however, represent the joint density of states multiplied by the transition probability, which is usually expressed by a matrix element like $\langle\psi_i|\nabla\psi_f\rangle$, where ψ_i and ψ_f are the wavefunctions of the initial and final states, respectively. We think that the matrix element effect is more important for TMTC's as compared with the dichalcogenides because the pure chalcogen p bands such as σ_g and σ_u^* bands are included in the valence and conduction bands. If the σ_g-σ_u^* band transitions occur, they would give rise to a peak around 7 eV.

TABLE I

MAIN ENERGY DISTANCES

	TiS_3	ZrS_3	HfS_3	NbS_3	TaS_3
O–A′	1.2	1.0	1.2	2.2	—
A″	—	—	2.7	—	—
A	2.0	2.7	3.4	1.4	2.4
B	4.8	5.6	6.0	5.0	5.6
C′	—	—	—	—	8.6
C	10	10	10	10	11.2
D	16	14.6	14	14.4	16.6
a–O	2.9	2.9		3.2	
A	4.8	5.6		4.6	
B	7.6	8.5		8.0	
C	14	13		13	
a′–O	6.0	6.0		6.0	
A′	7.2	7.0		8.2	
B	10.8	11.6		11.0	
b–O	9.4	8.8		9.3	
A	11.4	11.4		10.6	
B	14	14.6		14.4	
c–O	13	12.4		13	

Note. The symbol O represents the absorption edge.

(2) *The Group V Compounds*

The S K absorption spectrum of NbS_3 is shown in Fig. 5, together with the photoemission spectrum measured by Endo *et al.* (*14*) and the density of states calculated by Bullett (*8*). In this case, since the S K absorption overlaps the Nb L_{II} absorption, the spectrum was obtained in the ways previously used for the S K absorption spectrum of NbS_2 (*26*). The density of states diagram has been plotted on the figure by fitting the peak positions to those of the photoemis-

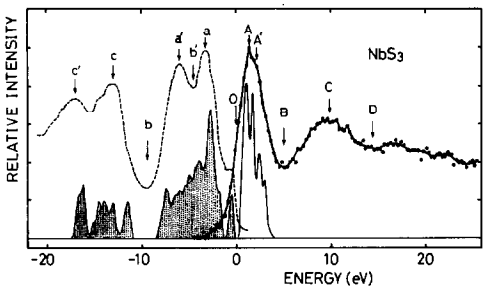

FIG. 5. S K absorption spectrum of NbS_3, together with the photoemission spectrum measured by Endo *et al.* (Ref. (*14*)) and the density of states calculated by Bullett (Ref. (*8*)). The full and dashed lines refer to the S K absorption and photoemission spectra, respectively.

sion spectrum as well as possible, and the S K absorption spectrum has been plotted on the figure by fitting the peak position to that of the density of states. The origin of the horizontal axis is the Fermi level determined from the photoemission study, which almost coincides with the absorption edge. The photon energy at the edge was estimated to be 2469.2 eV.

NbS_3 crystallizes in the isostructure of the group IV compounds, but Nb atoms are shifted from the mirror planes of the surrounding bicapped trigonal prisms to form the Nb–Nb pairs along the chain axis (*31*). This variation in crystal structures leads to the formation of the bonding $\sigma_g(d_{z^2}\text{-}d_{z^2})$ and

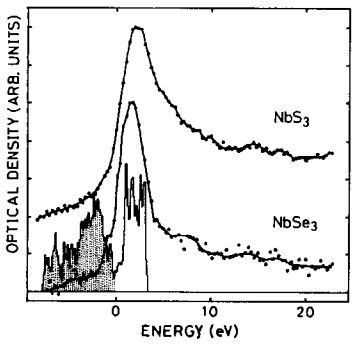

FIG. 6. Nb L_{III} absorption spectra of NbS_3 and $NbSe_3$. The density of states of $NbSe_3$ has been calculated by Bullett (Ref. (*7*)).

the antibonding $\sigma_u^*(d_{z^2}\text{-}d_{z^2})$ bands. The former band is pulled down just below the Fermi level, while the latter band shifts to higher energies compared with the other d bands unless the interaction is small. We expect that the sulfur antibonding $\sigma_u^*(p_x\text{-}p_x)$ and the metal d bands lie at the energy positions similar to those of TiS_3 because the sulfur pair distance is 2.05 Å, approximately equal to that of TiS_3, and the metal d levels are comparable for both compounds. Since the K absorption spectrum does not exhibit the antibonding d_{z^2} band, the overall appearance is expected to be similar to that of TiS_3, in agreement with the experimental result.

The metal L_{III} absorption spectrum of NbS_3 is shown in Fig. 6. Comparing with the Zr L_{III} absorption spectrum of ZrS_3, we find that the shoulder structure observed near the Zr L_{III} absorption edge vanishes and the other one appears at the higher energy side of the peak. Then we may assign it to the antibonding d_{z^2} band.

The Nb L_{III} absorption spectrum of $NbSe_3$ exhibits a peak sharper than that of the sulfide and than expected from the band calculation as shown in Fig. 6. The density of states of $NbSe_3$ has been calculated by Bullett (*7, 9*). A $NbSe_3$ crystal contains three types of trigonal chains which may be distinguished according to the degree of Se_2 pairing and then the unit cell is made up of the six trigonal prisms. The overall appearance resembles the metal L_{III} absorption spectrum of $ZrSe_3$ except for the near edge structures. This may imply that the energy band structures of these compounds depend predominantly on the neighbor surroundings. It is, however, important to note that, according to the band calculations of Bullett (*7*) and Hoffmann *et al.* (*10*), the lowest conduction band of $NbSe_3$ consists of the d_{z^2} band, unlike $ZrSe_3$.

Figure 7 shows the S K absorption spectrum of TaS_3. The overall appearance resembles that of TiS_3 and NbS_3, but in this

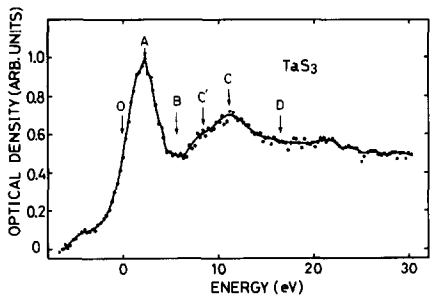

FIG. 7. S K absorption spectrum of TaS_3.

case the higher energy peak has a shoulder around 8.6 eV above the edge. At present we cannot discuss it in detail because the crystal structure is face-centered orthorhombic but not yet fully determined.

(3) *Core-Hole Potential and Core-Level Splitting*

The X-ray absorption process includes the core-electron excitations and the resulting core-hole potential may more or less affect the conduction and the valence states. The effects have recently been reviewed and discussed by Balzarotti *et al.* (*32*) and Grunes (*33*). In the previous X-ray absorption study of layered transition-metal dichalcogenides (*26*), however, they were assumed to be negligible because the spectra were not inconsistent with the results of the band calculations and with the other optical data. This assumption would also be reasonable for the present systems which are akin to the layered transition-metal dichalcogenides.

The S $2p$ and Se $3d$ photoemission studies of TiS_3, ZrS_3, and $ZrSe_3$ have, on the other hand, shown the level splitting probably due to the inequivalent S or Se atoms (*12, 16*). If the splitting also occurs in the S $1s$ level, then the S K absorption spectra would exhibit the overlapping structures of two absorptions, each of which is caused by the different kinds of S $1s$ electrons. Since the lower empty bands consist of the antibonding p band derived from the S pairs and of the metal nonbonding d_{z^2} band, their absorption structures would not be affected by the S $1s$ level splitting, while the metal d, s, and p bands are common for both the unpaired and paired S atoms, so that their absorption structures would be, respectively, observed as a doublet, its separation depending on the degree of the level splitting. Although the S K absorption spectrum of HfS_3 shows the additional peaks compared with that of ZrS_3, we can not conclude that these structures are caused by the core-level splitting because there have been no S $1s$ photoemission studies and no band calculations. On the other hand, the fact that the shape of the S K absorption spectrum of NbS_3, which does not show the doublets, is similar to that of the density of states, implies that the S $1s$ level splitting is not so large. This is supported by the S K absorption spectra of a series of titanium sulfides TiS_x (x = 1, 3/2, 2, 3). As shown in Fig. 8, the absorption edge is shifted to lower energies with x or with decreasing the negative charges around a S nucleus, although the trisulfide has the higher energy

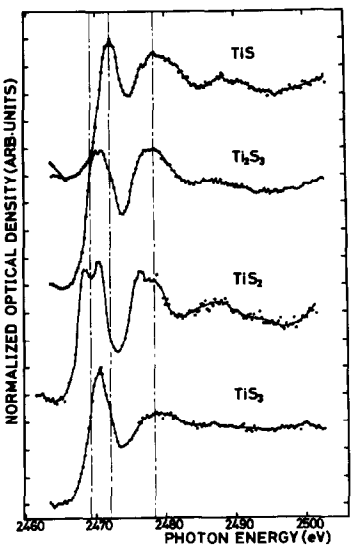

FIG. 8. S K absorption spectra of a series of titanium sulfides.

value than the disulfide. It is found from the above fact that the edge shifts of S K absorption spectra of these compounds are caused mainly by the filling of the empty bands or by the Fermi-level positions, but are not caused by the chemical shift of the S $1s$ level.

Conclusions

We have measured the sulfur K and metal L_{III} absorption spectra of TMTC's. Although the core-level photoemission studies of TiS_3 and ZrS_3 showed that the sulfur $2p$ levels are split into two peaks by the difference in atomic occupations (*12, 16*), the present authors think that this effect is not so strong for the $1s$ level due to the screening of the outer electrons and the spectra exhibit the conduction band structures sufficiently. The S K absorption spectra are similar to each other, but not to the corresponding metal L_{III} absorption spectrum. This is probably due to the matrix element effect and suggests that the lower conduction bands consist of the pure chalcogen p states (the antibonding $\sigma_u^*(p_x\text{-}p_x)$ band) and the pure metal d states (the nonbonding d_{z^2} band) in addition to the mixture states of chalcogen p and metal d states (the metal d bands). We have given the evidence that the lowest conduction band of the group IV TMTC's is the antibonding $\sigma_u^*(p_x\text{-}p_x)$ band which overlaps the nonbonding d_{z^2} band. We have also found that the overlap of the metal d and metal s bands is promoted by increasing the atomic number of chalcogen atoms.

Acknowledgment

This work was partially supported by a Grant in Aid for Scientific Research from the Ministry of Education of Japan.

References

1. J. ROUXEL, "Physics and Chemistry of Materials with Layered Structures" (F. Lèvy, Ed.), Vol. 6, p. 237, Reidel, Dordrecht/Boston/London (1979).
2. P. MONCEAU, N. P. ONG, A. M. PORTIS, A. MEERSHAUT, AND J. ROUXEL, *Phys. Rev. Lett.* **37,** 602 (1976).
3. N. P. ONG AND J. W. BRILL, *Phys. Rev. B* **18,** 5265 (1978).
4. J. CHAUSSY, P. HAEN, J. C. LASJAUNIAS, P. MONCEAU, G. WAYSND, A. WAINTAL, A. MERSCHAUT, P. MOLINIÉ, AND J. ROUXEL, *Solid State Commun.* **20,** 759 (1976).
5. T. SAMBONGI, K. TSUTSUMI, Y. SHIOZAKI, M. YAMAMOTO, K. YAMAYA, AND Y. ABE, *Solid State Commun.* **22,** 729 (1977).
6. D. W. BULLETT, *Solid State Commun.* **26,** 563 (1978).
7. D. W. BULLETT, *J. Phys. C* **12,** 277 (1979).
8. D. W. BULLETT, *J. Solid State Chem.* **33,** 13 (1980).
9. D. W. BULLETT, *J. Phys. C.* **15,** 3069 (1982).
10. R. HOFFMANN, S. SHAIK, J. C. SCOTT, M. H. WHANGBO, AND M. J. FOSHEE, *J. Solid State Chem.* **34,** 263 (1980).
11. H. W. MYRON, B. N. HARMAN, AND F. S. KHUMALO, *J. Phys. Chem. Solids* **42,** 263 (1981).
12. F. JELLINEK, P. A. POLLAK, AND M. W. SHAFER, *Mater. Res. Bull.* **9,** 845 (1974).
13. G. MARGARITONDO, A. D. KATNANI, AND N. G. STOFFEL, *J. Electron Spectrosc. Relat. Phenom.* **20,** 69 (1980).
14. K. ENDO, H. IHARA, K. WATANABE, AND S. GONDA, *J. Solid State Chem.* **39,** 215 (1981).
15. K. ENDO, H. IHARA, S. GONDA, AND K. WATANABE, *Physica B* **105,** 159 (1981).
16. K. ENDO, H. IHARA, K. WATANABE, AND S. GONDA, *J. Solid State Chem.* **44,** 268 (1982).
17. T. X. ZHAO, A. O. KANTANI, P. PERFETTI, AND G. MARGARITONDO, *Nuovo Cimento Soc. Ital. Fis. D* **1,** 549 (1982).
18. F. S. KHUMALO AND H. P. HUGHES, *Phys. Rev. B* **22,** 2078 (1980).
19. F. S. KHUMALO, C. G. OLSON, AND D. W. LYNCH, *Physica B* **105,** 163 (1981).
20. W. H. G. GRIMMEISS, A. RABENAU, H. HAHN, AND P. NESS, *Z. Electrochem.* **65,** 776 (1961).
21. W. SCHARER AND M. W. SHAFER, *Phys. Status Solidi A* **17,** 181 (1973).
22. G. PERLUZZO, S. JANDL, AND P. E. GIRALD, *Canad. J. Phys.* **58,** 143 (1980).
23. S. KURITA, J. L. STAEHLI, M. GUZZI, AND F. LÉVY, *Physica B* **105,** 169 (1981).
24. F. K. MCTAGGART AND A. D. WADSLEY, *Aust. J. Chem.* **11,** 445 (1958).

25. Y. OHNO, H. WATANABE, A. KAWATA, S. NAKAI, AND C. SUGIURA, *Phys. Rev. B* **25,** 815 (1982).
26. Y. OHNO, K. HIRAMA, S. NAKAI, C. SUGIURA, AND S. OKADA, *Phys. Rev. B* **27,** 3811 (1983).
27. G. PERLUZZO, A. A. LAKHANI, AND S. JANDL, *Solid State Commun.* **35,** 301 (1980).
28. S. FURUSETH, L. BRATTÅS, AND A. KJEKSHUS, *Acta Chem. Scand. A* **29,** 623 (1975).
29. B. M. DAVIES AND F. C. BROWN, *Phys. Rev. B* **25,** 2997 (1982).
30. Y. OHNO, in press.
31. J. RINSDORP AND F. JELLINEK, *J. Solid State Chem.* **25,** 325 (1978).
32. A. BALZAROTTI, M. D. CRESCENZI, AND L. INCOCCIA, *Phys. Rev. B* **25,** 6349 (1982).
33. L. A. GRUNES, *Phys. Rev. B* **27,** 2111 (1983).